Melleolides impact fungal translation via Elongation Factor 2

Maximilian Dörfer,[a] Daniel Heine,[b] Stefanie König,[c] Sagar Gore,[d] Oliver Werz,[c] Christian Hertweck,[b] Markus Gressler,[a] Dirk Hoffmeister[a,*]

a Department Pharmaceutical Microbiology at the Hans Knöll Institute, Friedrich-Schiller-University, Beutenbergstrasse 11a, 07745 Jena, Germany
b Department Biomolecular Chemistry, Leibniz Institute for Natural Product Chemistry and Infection Biology - Hans Knöll Institute, Beutenbergstrasse 11a, 07745 Jena, Germany
c Department Pharmaceutical and Medicinal Chemistry, Friedrich-Schiller-University Jena, Philosophenweg 14, 07743 Jena, Germany
d Department Systems Biology and Bioinformatics, Leibniz Institute for Natural Product Chemistry and Infection Biology - Hans Knöll Institute, Beutenbergstrasse 11a, 07745 Jena, Germany
*Correspondence: Dirk Hoffmeister, Markus Gressler, Department Pharmaceutical Microbiology at the Hans Knöll Institute, Friedrich-Schiller-University, Beutenbergstrasse 11a, 07745 Jena, Germany; Phone: +49-3641-949851; Fax: +49-3641-949852; e-mail: dirk.hoffmeister@hki-jena.de, markus.gressler@hki-jena.de.

Electronic supplementary information

Table of contents

Table S1. NMR data of **5** in CD_3OD. [a]3-OH and 3'-OH not observed; [b] not assigned due to signal overlap.

no.	δ_C, type	δ_H (*J* in Hz)	HMBC
1	192.6, CH	9.86 s	1, 2, 3, 4
2	134.6, qC		
3	73.3, CH[a]	4.31 dd (2.3; 7.3)	2, 4, 9
4	169.5, qC		
5	71.3, CH	6.33 m	2, 4, 6
6	46.3, CH_2	a: 2.15 dd (5.8; 9.4) b: 2.74 dd (6.9; 9.3)	b: 4, 8, (1') a: 5, 6
7	41.1, qC		
8	21.3, CH_3	1.20	4, 6, 7
9	47.6, CH	2.48 m	8, (3), (6), (11)
10	41.9, CH_2	1.53-1.42 m	10, 13, 14, 15
11	40.6, qC		
12	47.4, CH_2	a: 1.24 dd (9.0; 10.3) b: 1.84 m	b: 9, 15 a: 3, 15
13	50.2, CH	2.34-2.38 m	3, 12
14	29.9, CH_3	1.12 s	9, 11, 15
15	27.6, CH_3	1.00 s	9, 11, 14
1'	169.8, qC		
2'	114.9, qC		
3'	161.8, qC[a]		
4'	108.8, CH	6.52 d (2.0)	3', 5', 6'
5'	155.3, qC		
6'	116.7, CH	6.49 d (1.9)	2', 4', 5', 8'
7'	142.4, qC		
8'	22.3, CH_3	2.40 s	6', 7'
1''	172.7, qC		
2''	34.2, CH_2	2.61	1", 3", 4"
3''	25.5, CH_2	2.07	1", 2", 4", 5"
4''	25.6, CH_2	2.81	2", 3", 5", 6"
5''	147.9, qC		
6''	124.4, CH	7.83 s	
I	41.2, CH_2	a) 2.66 m b) 2.88 dd (4.3; 10.6)	II, VII, VI
II	61.6, CH	4.45 m	I, IV, VII
III	NH	6.20	
IV	166.1, qC		
V	NH	6.16	
VI	63.3, CH	4.25 m	I, IV, VII
VII	57.0, CH	3.15 m	IX, X
VIII	26.8, CH_2	1.62 m	VI, IX, X, XI
IX	29.8, CH_2	1.40 m	VII, XI
X	29.5, CH_2	1.67-1.72 m	IX, (VII)
XI	36.7, CH_2	2.18 t (6.0)	
XII	176.1, qC		
XIII	NH	8.45	
XIV	40.3, CH_2	3.31 m	XVI-XIX, XII
XV	70.6, CH_2	3.48 t(4.63)	XIV, XVI-XIX
XVI[b] **XVII**[b] **XVIII**[b] **XIX**[b]	71.5 – 71.2, 4 x CH_2	3.54-3.59 m	XVI-XIX
XX	70.4, CH_2	3.85 m	XXI, XIX
XXI	51.4, CH_2	4.55 m	XX, C6"

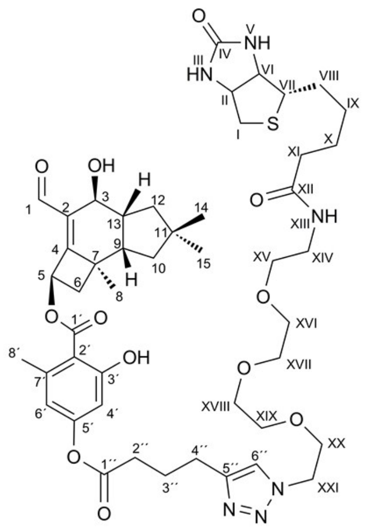

Table S2. NMR data of **6** in CD_3OD. [a]not assigned due to signal overlap.

no.	δ_C, type	δ_H (*J* in Hz)	HMBC
1	14.1, CH_3	0.98 t (7.4)	2, 3
2	19.8, CH_2	1.47 sext (7.5)	3, 4, 1
3	31.3, CH_2	1.74 quin (6.6)	1, 2, 4
4	65.5, CH_2	4.30 t (6.6)	2, 3, 1'
1'	166.3, qC		
2'	128.8, qC		
3'	131.5, CH	8.05 d (8.7)	7', 6', 4', 5', 2'
4'	122.2, CH	7.17 d (8.7)	6', 2', 5', 1', (1'')
5'	154.9, qC		
6'	122.2, CH	7.17 d (8.7)	4', 2', 5', 1', (1'')
7'	131.5, HC	8.05 d (8.7)	3', 6', 4', 5' 2'
8'			
1''	172.0, qC		
2''	34.1, CH_2	2.67 t (7.5)	1'', 3'', 4''
3''	25.1, CH_2	2.12 m	1'', 2'', 4'', 5''
4''	25.3, CH_2	2.83 t (7.5)	2'', 3'', 6''
5''	147.3, qC		
6''	122.7, CH	7.55 s	5''
I	41.1, CH_2	a) 2.71 s b) 2.90 dd (5.1; 7.8)	II, VI, VII II
II	60.7, CH	4.47 m	I, VII, IV (VI)
III	NH	6.02	
IV	164.1, qC		
V	NH	6. 2	
VI	62.3, CH	4.30 m	I, VII, IV, (II)
VII	56.0, CH	3.15 dt (4.6; 7.4)	IX, X
VIII	26.1, CH_2	1.64 m	VII, VI, IX, X, XI
IX	28.6, CH_2	1.43 m	VIII, X, XI, VII
X	28.6, CH_2	1.62-1.75 m	
XI	36.3, CH_2	2.18 t (7.5)	X, IX, VIII, XII
XII	173.4, qC		
XIII	NH	6.43 s	XII
XIV	39.8, CH_2	3.38 quar (5.2)	XV, XII
XV	70.4, CH_2	3.51 t (5.2)	XVI-XIX, XIV
XVI[a] **XVII**[a] **XVIII**[a] **XIX**[a]	71.2-70.7, 4 x CH_2	3.55-3.60 m	XVI-XIX
XX	70.1, CH_2	3.86 t (5.2)	XXI, XVI-XIX
XXI	50.8, CH_2	4.51 t (5.2)	XX, C6"

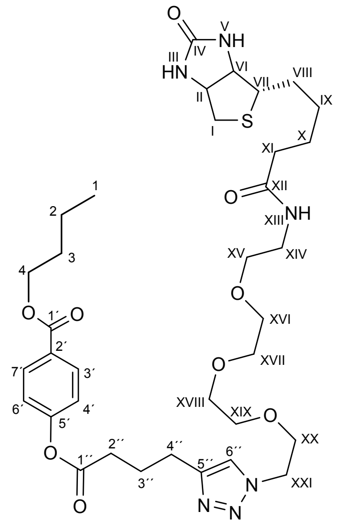

Table S3. MALDI-TOF-based peptide identification of eEF1α and eEF2 in protein fractions after elution from 5-labelled streptavidin beads. The sequence coverage (SC) and the root mean square at 90% (RMS90), which is used to compare distributions without large non-gaussian tails dominating, are indicated.

band no.	identified protein	pI	MW [kDa]	Meta Score	Peptides	SC [%]	RMS90 [ppm]
1	TPA: elongation factor 1-alpha (eEF 1α) [*Aspergillus nidulans* FGSC A4]	9.9	50.5	55.0	5	15.0	5.87
2	EF2_NEUCR Elongation factor 2 (eEF 2) [*Aspergillus nidulans* FGSC A4]	6.2	93.8	199.0	19	29.4	10.38

Table S4. **Molecular fingerprint (FP) similarity analysis of 1 and 7 by encoding them into Morgan and 2D Pharmacophore FPs.** Tanimoto similarity values higher than 0.5 could be used as cut-off for similarity when Morgan FPs are used. Dice coefficients may have a higher cut-off depending on the FPs used to encode the given molecules.

Similarity metric	2D Pharmacophore	Morgan
Tanimoto	0.147	0.164
Dice	0.257	0.283

Table S5. Predicted binding pockets for 1 in *A. nidulans* eEF2 model by the Achilles blind docking server. Ranks for the first seven binding pockets are given along with their predicted free energies of binding (BE). 5 Å residues around the predicted binding coordinates for **1** in *A. nidulans* eEF2 are listed. Residue numbering is shown in accordance with *A. nidulans* eEF2 (*An*), *C. albicans* eEF2 (*Ca*) and *S. cerevisiae* eEF2 (*Sc*). Amino acid residues differences are highlighted in bold.

#	BE	organ.	5 Å residues from predicted DAO binding location
1	-8.3	*An*	466K 484FS 515SDPC 534**A**G 537LH 541IC 545D 550H 731F 795PQ**SV**
		Ca	K FS SDPC **T**G LH IC D H F PQ**LI**
		Sc	K FS SDPC **T**G LH IC D H F PQ**MV**
2	-7.5	*An*	171**E**KED 250**Y** 262**QPE** 267GKP**V**ER 275NM
		Ca	**T**KED **Y** **DKD** GKP**L**ER NM
		Sc	**S**KED **F** **DTD** GKP**L**ER NM
3	-7.5	*An*	418N 484FSVS 565R 600**K** 603E**E** 638GPD 643G**A**N 672T 681**PM**RS 799FDHW
		Ca	N FSVS R **L** E**N** GPD G**P**N T **NC**RS FDHW
		Sc	N FSVS R **L** E**N** GPD G**P**N T **EM**RS FDHW
4	-7.1	*An*	42**R** 79**AKFA** 86D 224RQF 228**VK** 305E 327KFLP 333ADA 336LE
		Ca	**K** **ASMT** D RQF **NK** E KFLP ADA LE
		Sc	**R** **SEMS** D RQF **TR** E KFLP ADA LE
5	-7.0	*An*	492**R** 536E 559**D**PVV 564Y 727E 752R 776NE 779F 805**L** 816K 819**Q**I 823**E**
		Ca	**V** E **P**PVV Y E R NE F **M** K **A**I **E**
		Sc	**V** E **P**PVV Y E R NE F **L** K **E**I **A**
6	-7.0	*An*	165LLE 169Q**VE**K 280D 283**YK** 286F**Q** 290**T**N
		Ca	LLE Q**TT**K D **FR** F**A** **M**N
		Sc	LLE Q**VS**K D **FR** F**T** **M**N
7	-7.0	*An*	226F 229**KF** 232KKF 251F 253P 276MFI 280DP 284**K** 303K**I**E
		Ca	F **KY** KKF F P MFI DP **R** K**L**E
		Sc	F **RY** KKF F P MFI DP **R** K**L**E

A

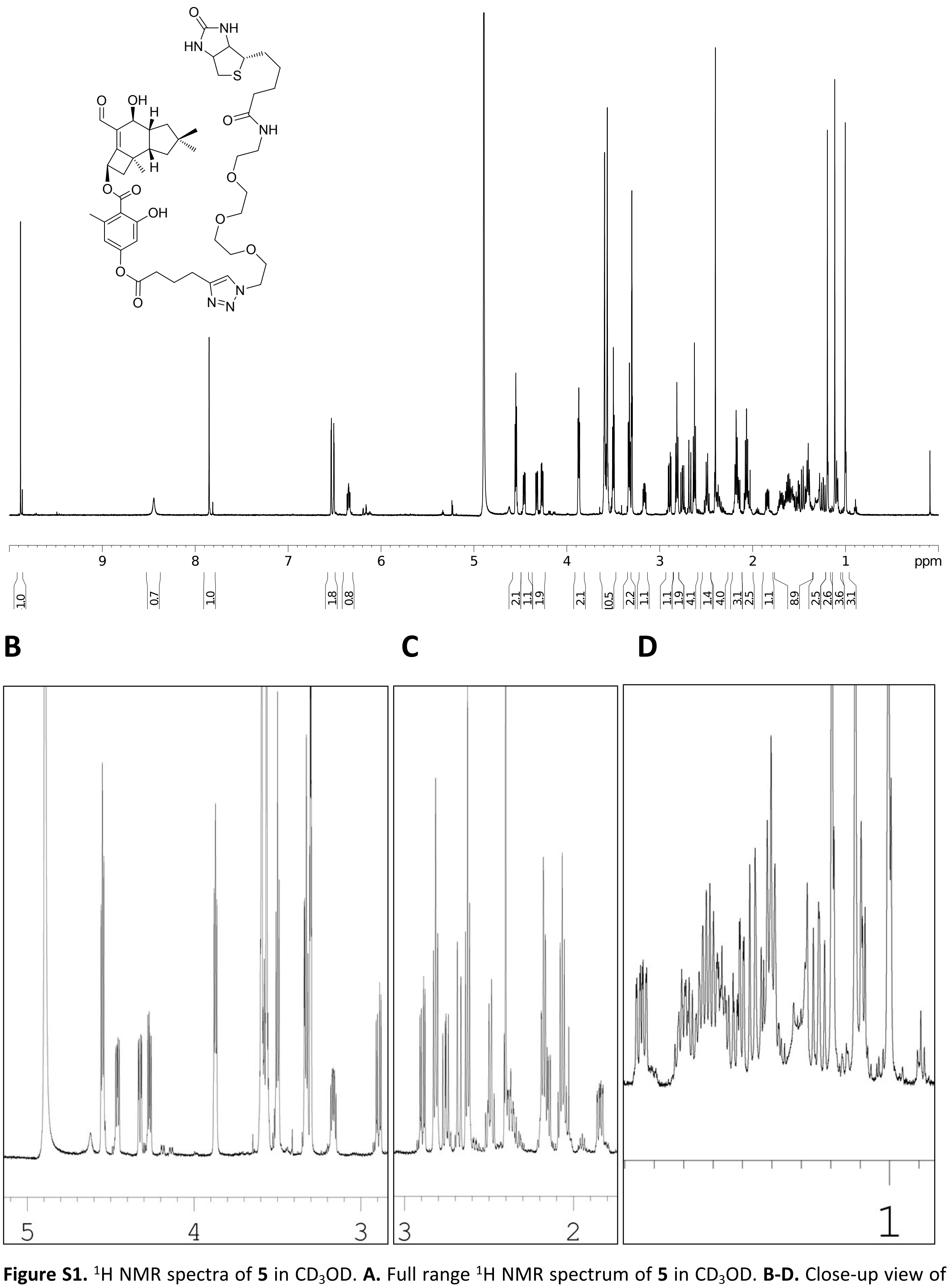

Figure S1. ^{1}H NMR spectra of **5** in CD_3OD. **A.** Full range ^{1}H NMR spectrum of **5** in CD_3OD. **B-D.** Close-up view of portions (5.0-3.0 ppm, 3.0-2.0 ppm, and 1.8-1.0 ppm) of the ^{1}H NMR spectrum of **5**.

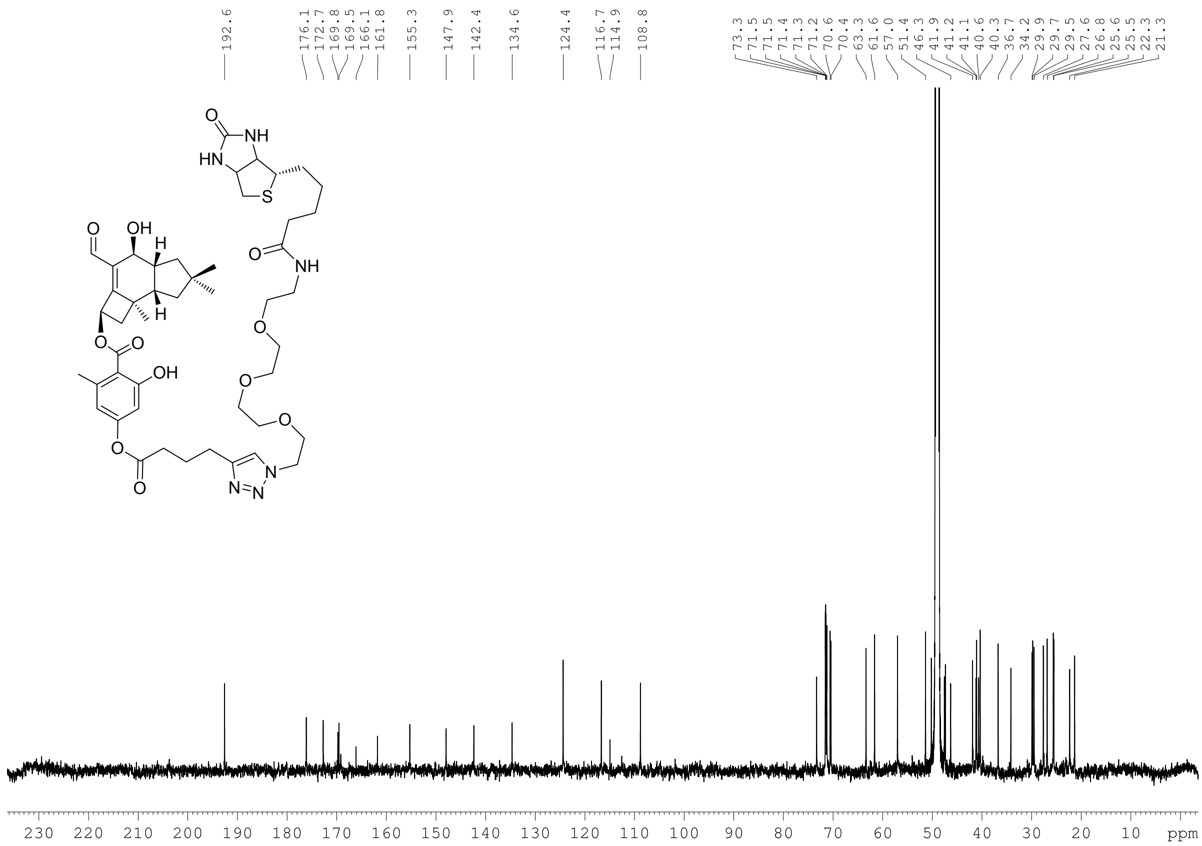

Figure S2. ^{1}H-decoupled ^{13}C NMR spectra of **5** in CD_3OD.

A

B

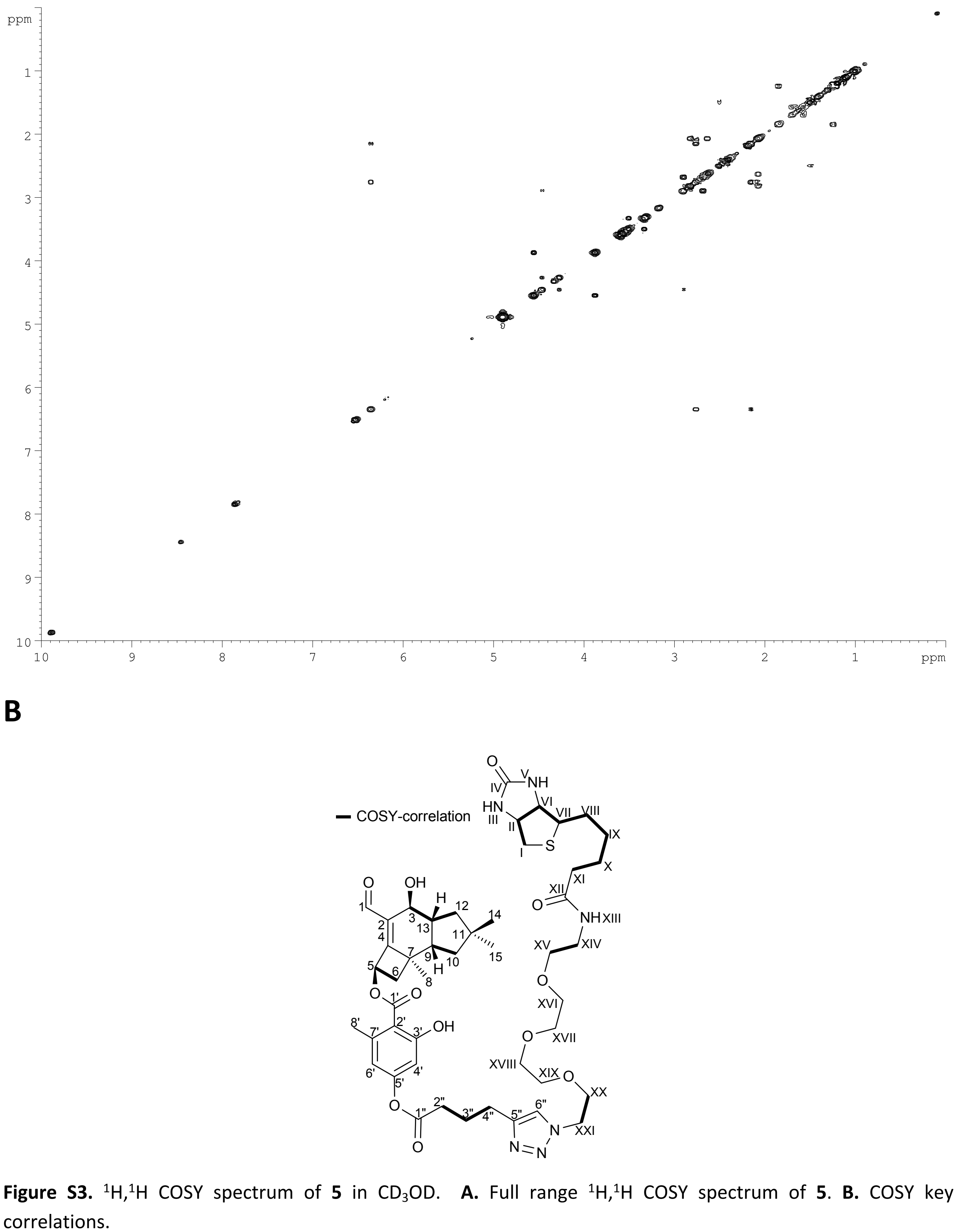

Figure S3. ^{1}H,^{1}H COSY spectrum of **5** in CD_3OD. **A.** Full range ^{1}H,^{1}H COSY spectrum of **5**. **B.** COSY key correlations.

A

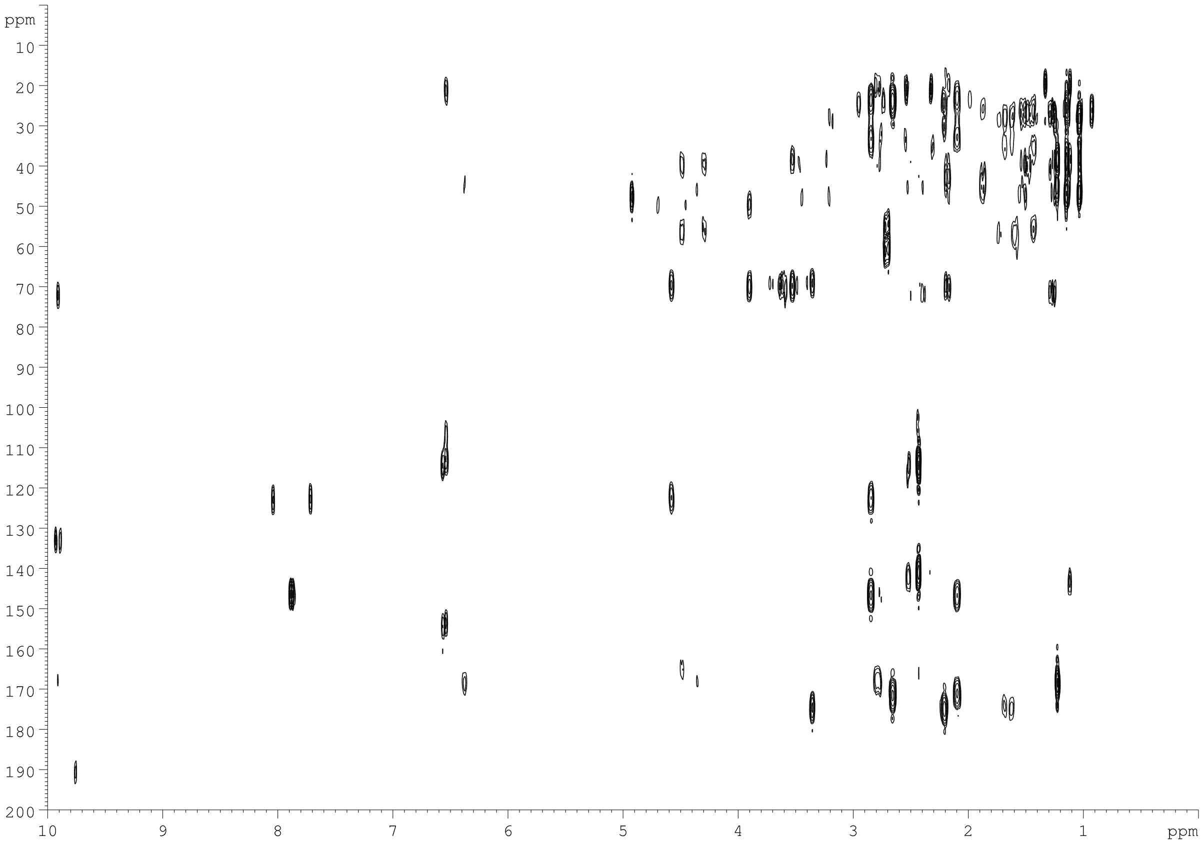

B

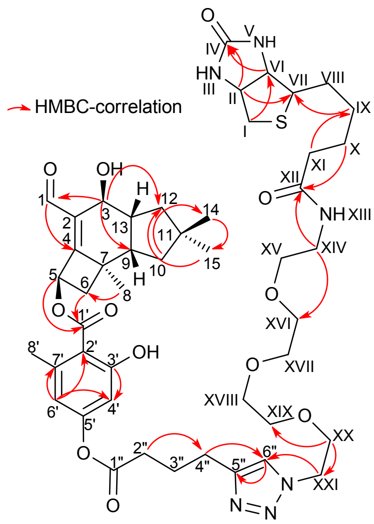

Figure S4. ^{1}H,^{13}C HMBC spectrum of **5** in CD_3OD. **A.** Full range ^{1}H,^{13}C HMBC spectrum of **5**. **B.** HMBC key correlations.

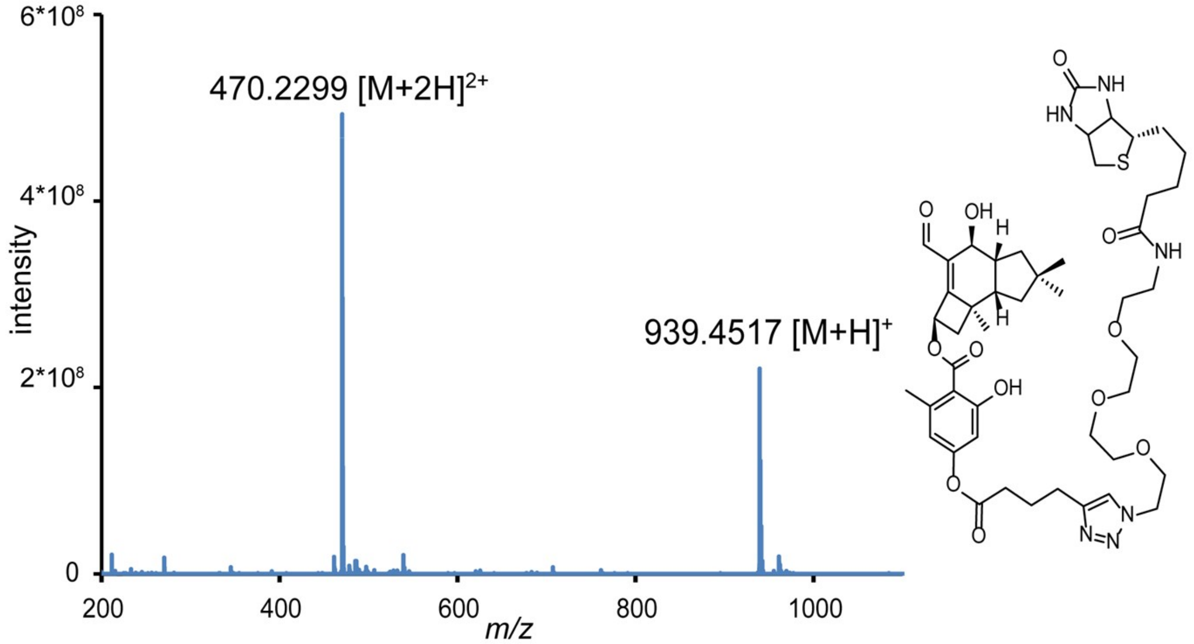

Figure S5. ESI-MS spectrum of **5**.

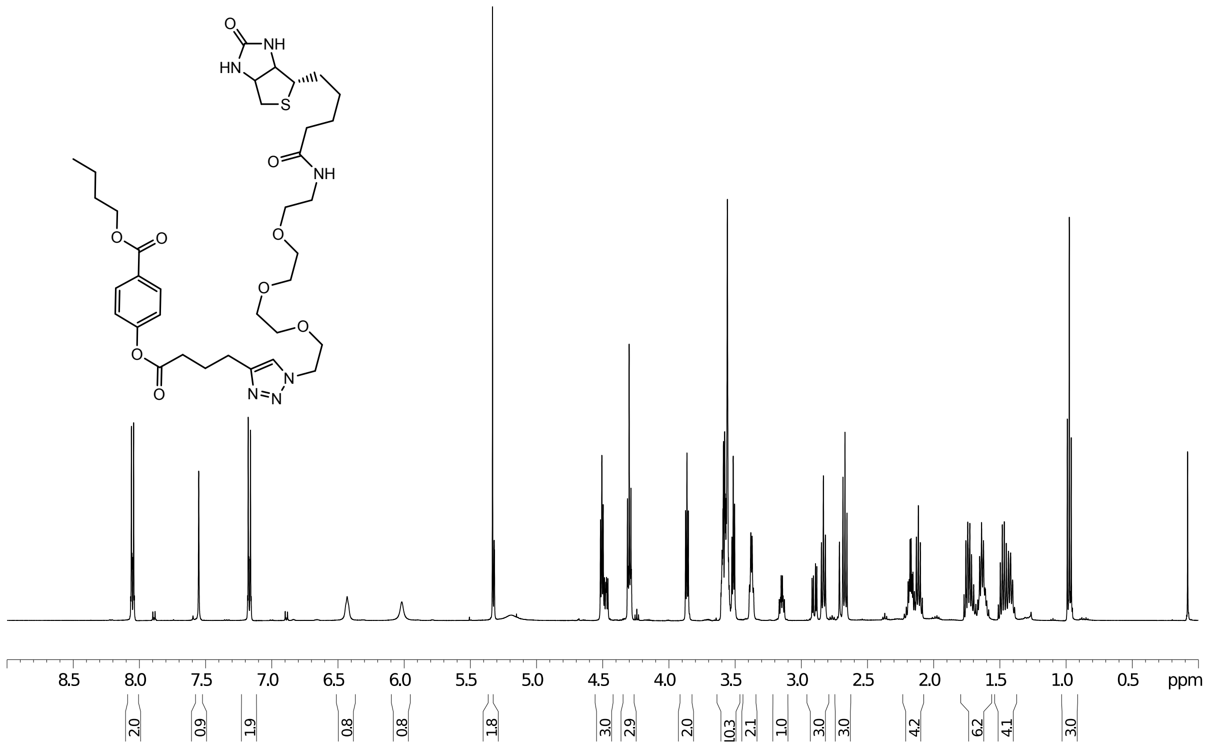

Figure S6. ^{1}H NMR spectrum of **6** in CD_3OD.

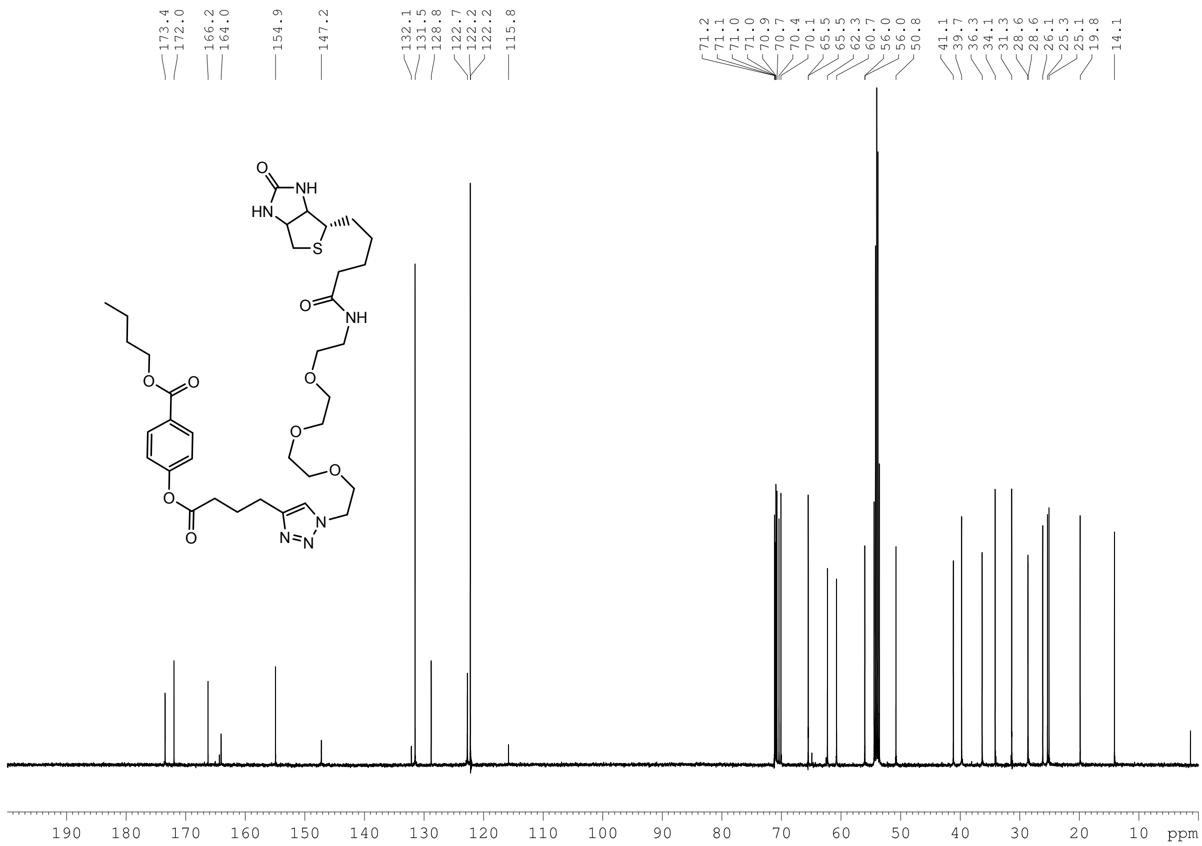

Figure S7. [1]H-decoupled [13]C NMR spectrum of **6** in CD_3OD.

A

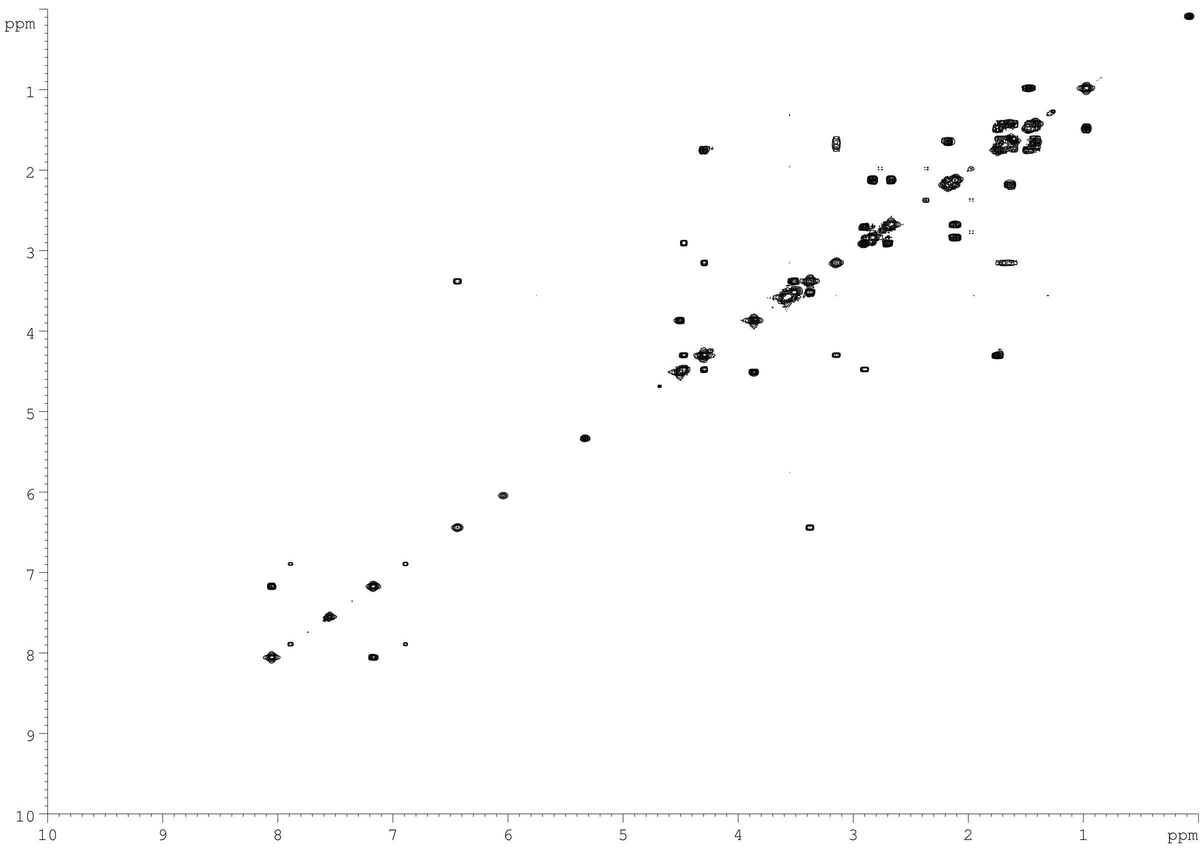

B

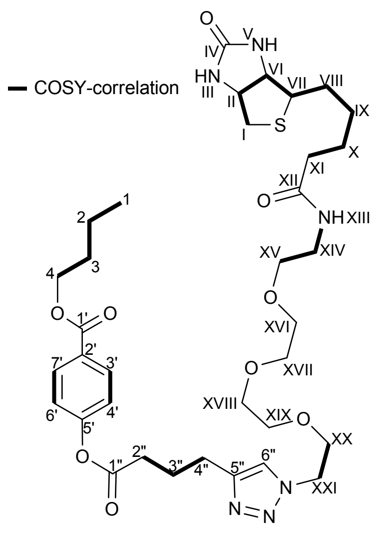

Figure S8. ^1H, ^1H COSY spectrum of **6** in CD_3OD. **A.** Full range ^1H, ^1H COSY spectrum of **6**. **B.** COSY key couplings in **6**.

A

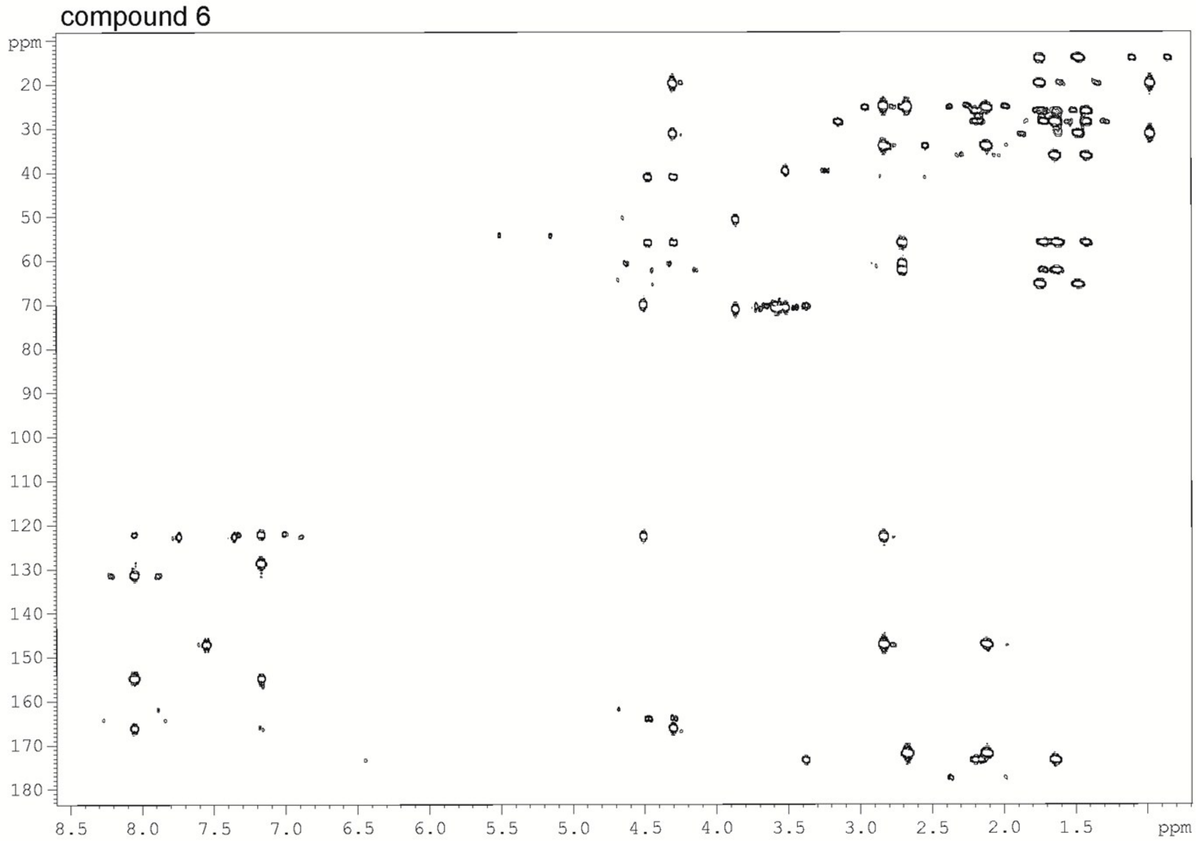

B

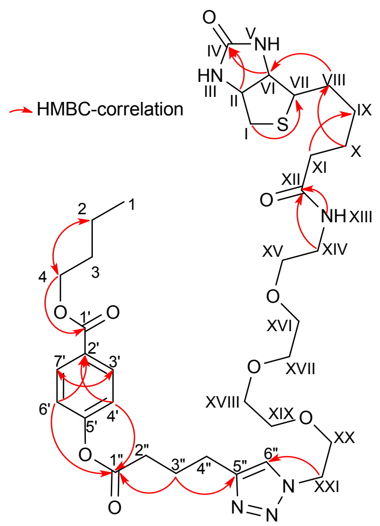

Figure S9. $^{1}H,^{13}C$ HMBC spectrum of **6** in CD_3OD. **A.** Full range $^{1}H,^{13}C$ HMBC spectrum. **B.** HMBC key correlations.

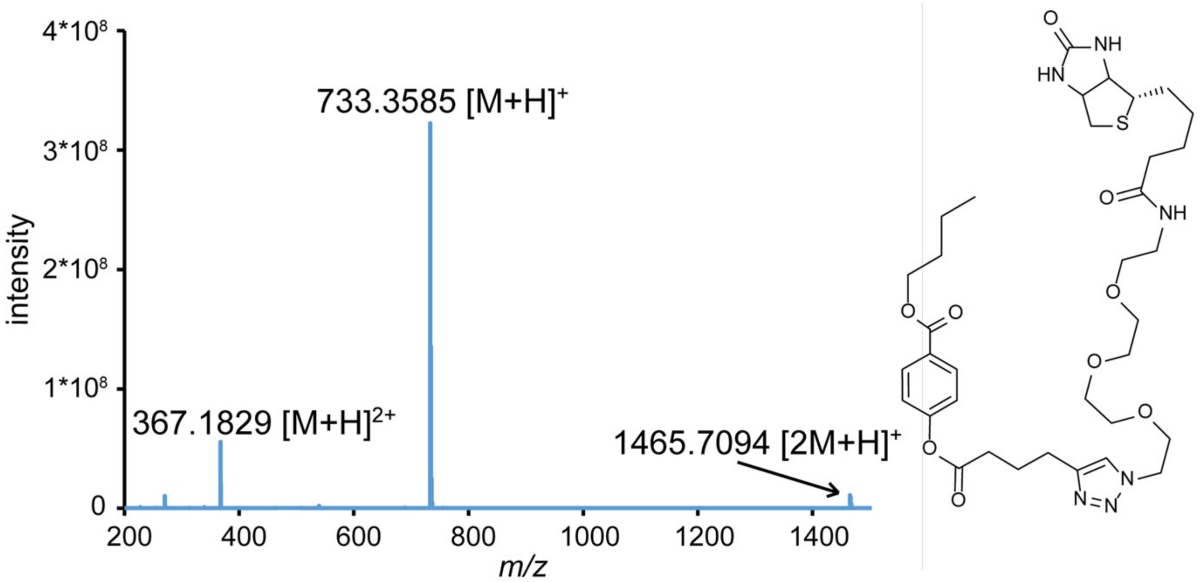

Figure S10. ESI-MS data of **6.**

Figure S11. MALDI-TOF-based peptide fingerprinting. Identified peptides from *A. nidulans* eEF2 in protein pull-down fraction with **5**-labelled streptavidin beads. Identified peptides from trypsin treated samples were aligned to *A. nidulans* eEF2 (highlighted in red). Grey bars indicate the reliance of the identified peptides: The darker the bar the lower is the difference between the measured *m/z* and the calculated *m/z*.

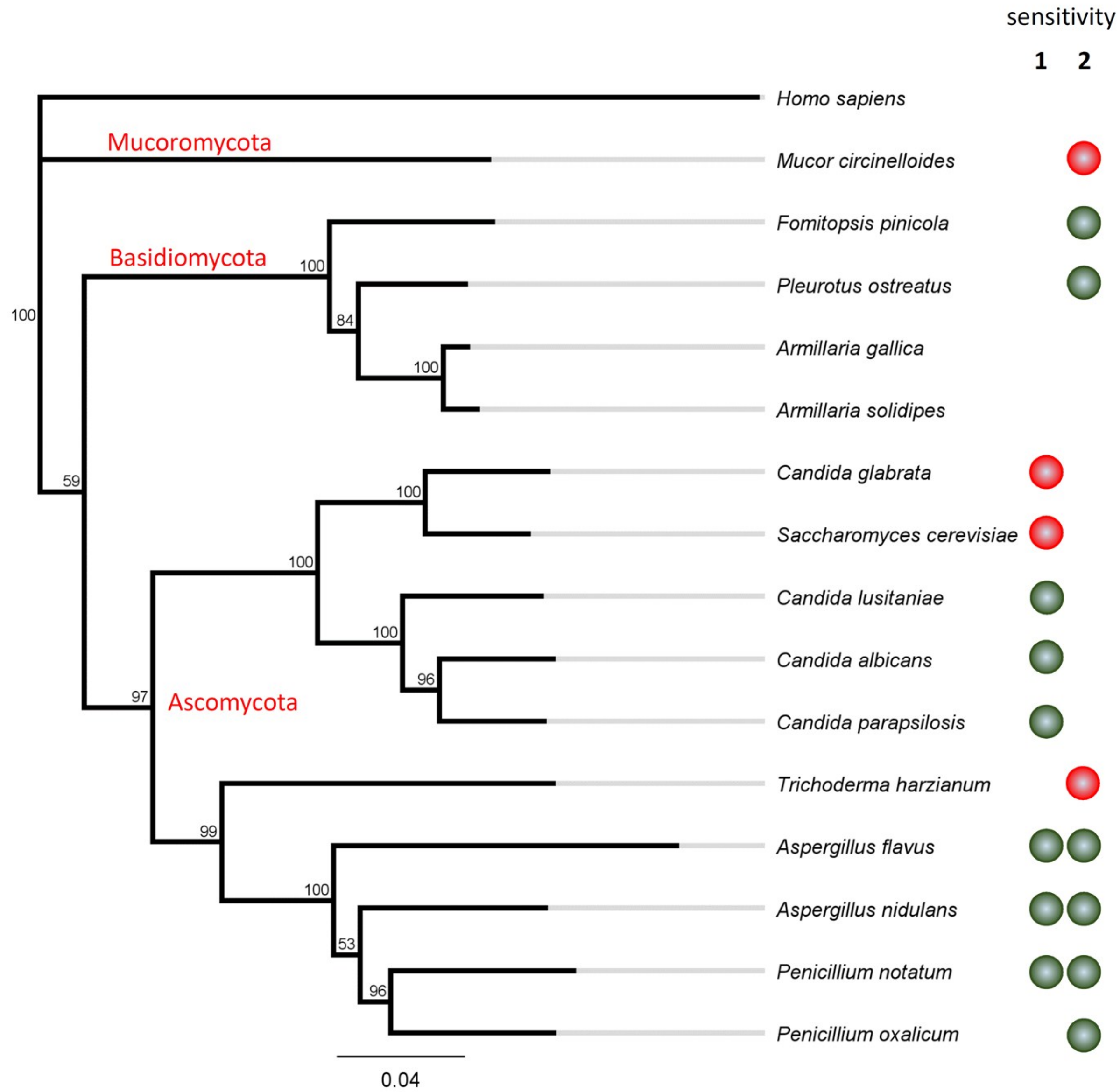

Figure S12. Phylogenetic analysis of fungal eEF2 with documented resistance or sensitivity towards 1 (DAO) and 2 (arnamial). Multiple amino acid sequence alignments were performed using the MUSCLE Alignment tool implemented in the Geneious 10.2.3 software carried out in default mode with a maximum of 1,000 iterations and 1,000 trees to be build. Phylogenetic analyses were performed with Geneious Tree Builder software using the Jukes-Cantor genetic distance model and the neighbour-joining method. The amino acid sequence of the human eEF2 was used as outgroup to root the tree. The bootstrap method was used as a resampling technique to estimate statistics on 1,000 replicates. Bootstrap values (consensus support in %) are given next to the branches in the consensus tree. Red and green spheres indicate resistance and sensitivity, respectively, towards **1** and **2** as reported by Misiek *et al.*[1], Bohnert *et al.*[2], and by this work (Figure 3 A).

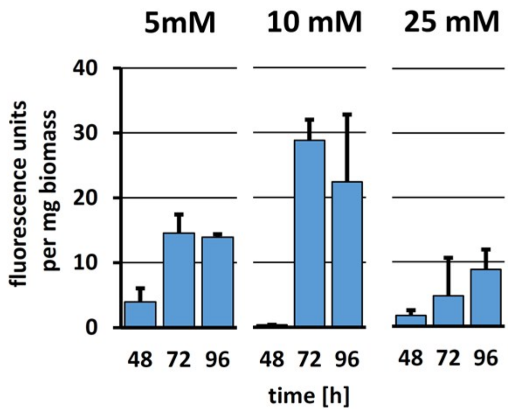

Figure S13. Optimization of cultivation conditions. *A. nidulans* tMD03 was cultivated for 48, 72, and 96 h in AMM containing 100 mM ethanol and 5, 10, or 25 mM D-glucose. Fluorescence units of cell-free total protein extracts were determined and normalised against the fungal biomass.

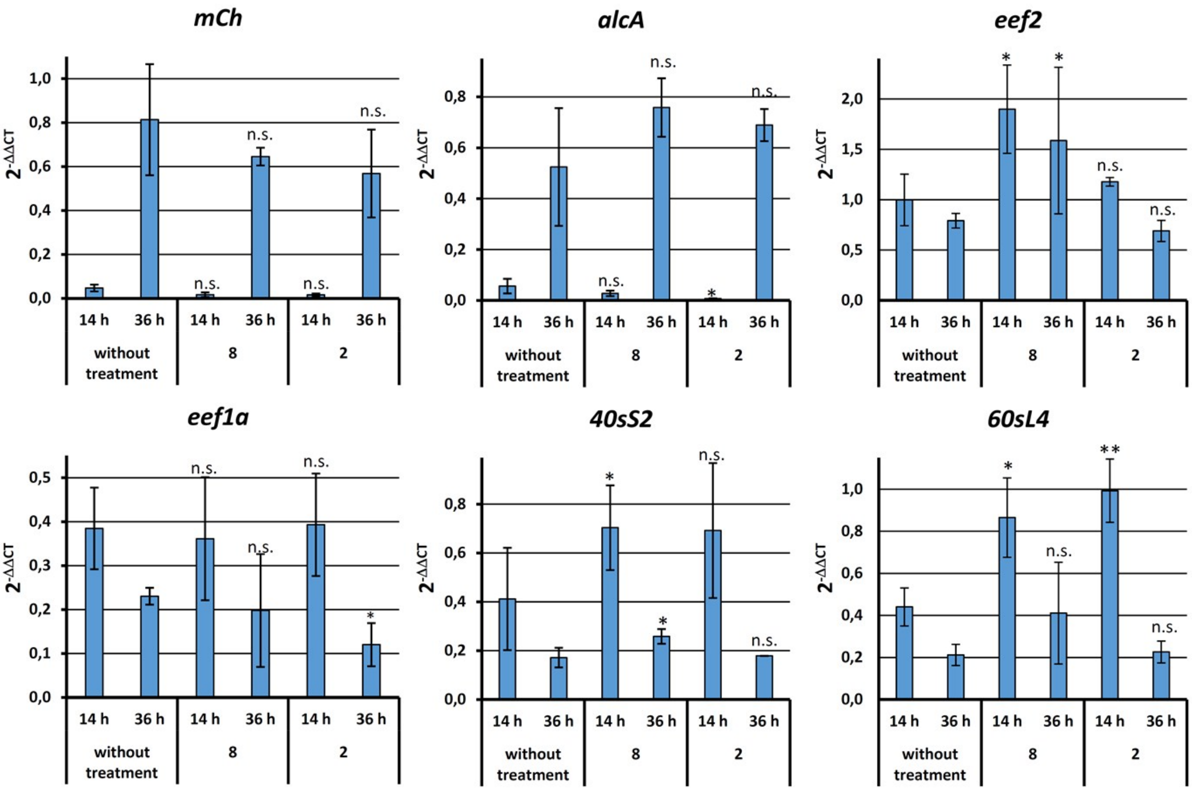

Figure S14. Gene expression analyses by qRT-PCR. *A. nidulans* tMD03 was pre-cultivated for 16 h in presence of 10 mM D-glucose and 100 mM ethanol. Compounds **8** (72 µM) or **2** (22 µM) were added, and cultures were grown for additional 14 or 36 h prior to expression analysis. Untreated cultures served as control. qRT-PCR targeted the genes for mCherry (*mCh*), alcohol dehydrogenase (*alcA*), eEF2 (*eef2*), eEF1α (*eef1α*), and proteins for the small (*40sS2*) and large (*60sL4*) ribosomal subunits. Expression levels were normalised against two housekeeping genes, i.e., enolase (*enoA*) and glycerinaldehyde-3-phosphate dehydrogenase (*gpdA*). Significance of gene expression levels were calculated against the respective untreated control by pairwise student´s t-test (n.s., $p > 0.05$; *, $p < 0.05$; **, $p < 0.01$).

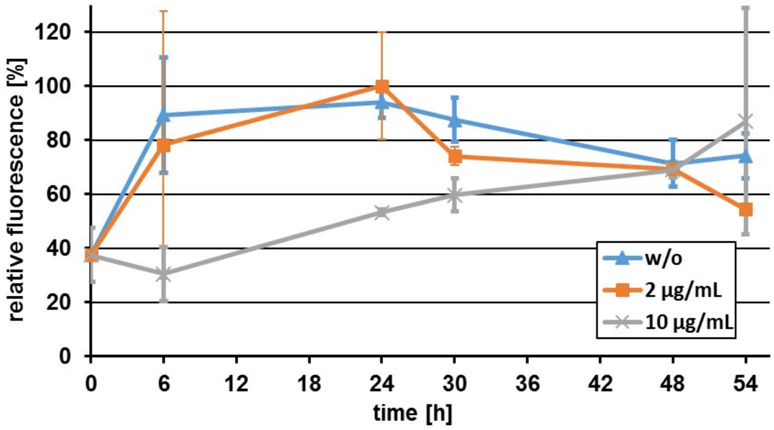

Figure S15. *In vivo* inhibition of protein biosynthesis in *A. nidulans* tMD03. The fungus was treated with **2** at 2 and 10 µg mL^{-1}. The untreated control served as internal fluorescence reference standard. The experiment was carried out as described in Figure 4.

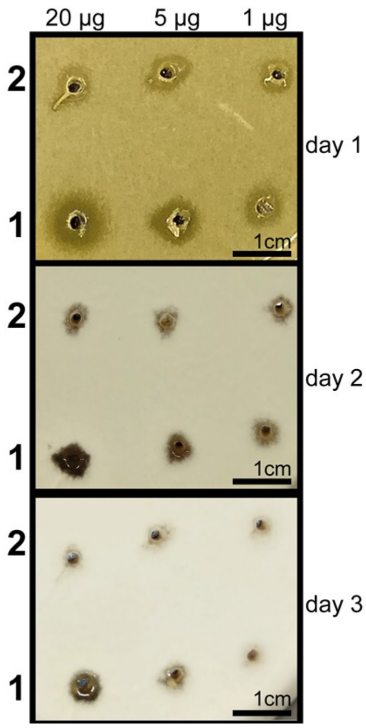

Figure S16. Recovery of *A. nidulans* in presence of 1 and 2. AMM plates were inoculated with *A. nidulans* FGSC A4 at a concentration of 1 x 10^6 conidia mL^{-1}, and 20, 5 or 1 µg of **1** and **2** were supplied. Plates were incubated for 1, 2, or 3 days at 30 °C. The size of inhibition zones is time-dependently reduced, indicating a fungistatic activity of **1** and **2**.

Scheme S1. Synthesis route for compound **6**.

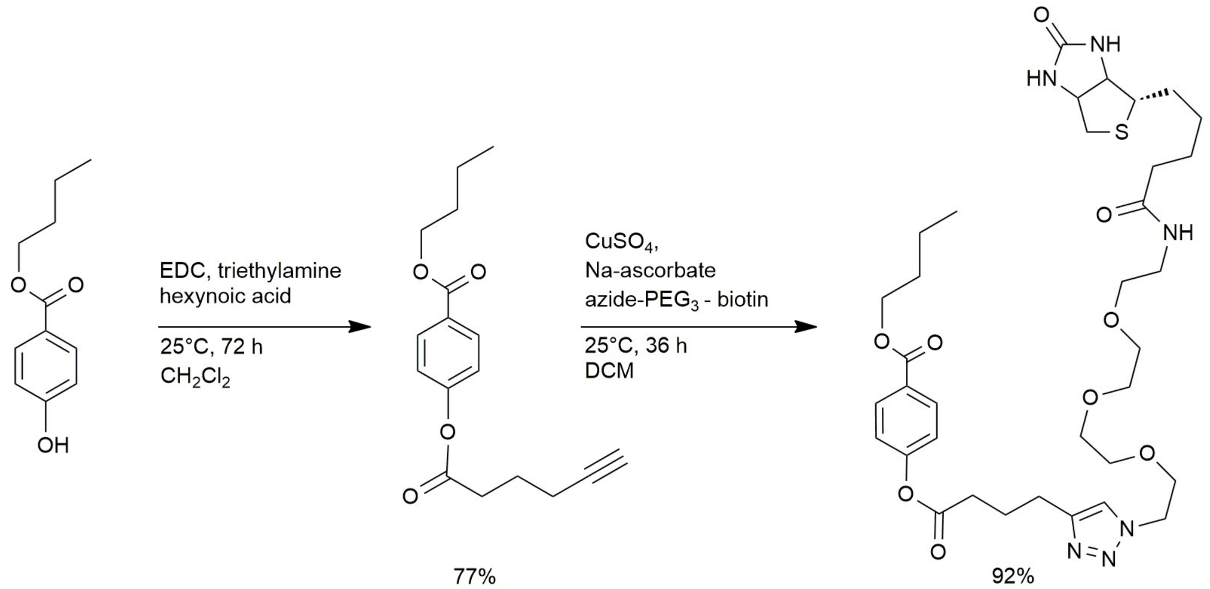

9 **6**

References

1. Misiek, M.; Hoffmeister, D. *Mycol. Prog.* **2012,** *11*, 7.
2. Bohnert, M.; Nützmann, H. W.; Schroeckh, V.; Horn, F.; Dahse, H. M.; Brakhage, A. A.; Hoffmeister, D. *Phytochemistry* **2014,** *105*, 101.